

Silicon nanowire and polyethylene superhydrophobic surfaces for discrete magnetic microfluidics

Ana Egatz-Gómez^a, John Schneider^a, P. Aella^b, Dongqing Yang^b,
P. Domínguez-García^c, Solitaire Lindsay^a, S.T. Picraux^{b,d}, Miguel A. Rubio^c,
Sonia Melle^{a,e}, Manuel Marquez^{a,f}, Antonio A. García^{a,*}

^aHarrington Department of Bioengineering, Arizona State University, Tempe, AZ 85287, USA

^bDepartment of Chemical and Materials Engineering, Arizona State University, Tempe, AZ 85287, USA

^cDepartamento de Física Fundamental, UNED, Madrid 28040, Spain

^dLos Alamos National Lab, Los Alamos, NM 87545, USA

^eDepartamento de Óptica, Universidad Complutense de Madrid, Madrid 28037, Spain

^fResearch Center, Philip Morris USA, Richmond, VA 23234, USA

Available online 20 July 2007

Abstract

A microfluidic method to manipulate small drops of water is studied on two different superhydrophobic surfaces. Using this digital magnetofluidic method, water drops containing paramagnetic carbonyl-iron microparticles were displaced on silicon nanowire (Si NW) and low-density polyethylene (LDPE) superhydrophobic surfaces using magnetic fields. Horizontal, vertical, or upside-down drop movement is made possible by the action of capillary forces induced by paramagnetic particles aligning and following a magnetic field, indicating that three-dimensional digital microfluidics is possible. Also, both Si NW and LDPE superhydrophobic surfaces combine surface chemistry with nano and microscale surface roughness to make drop movement possible. Si NW superhydrophobic surfaces were prepared using vapor–liquid–solid growth systems followed by coating with a perfluorinated hydrocarbon. LDPE superhydrophobic surfaces were prepared by growing polyethylene crystals on a polyethylene substrate through careful rate control.

© 2007 Elsevier B.V. All rights reserved.

PACS : 47.55.D; 47.55.dr; 81.07.–b; 87.83.+a

Keywords: LDPE; Polyethylene; Silicon nanowire; Microfluidic; Magnetofluidic

1. Introduction

Technological advances are bringing closer to reality decentralized “near-patient” or “point-of-care” testing for a wide spectrum of analytes [1], to provide fast quantitative results at the bedside, the physician’s office, emergency-rooms, or for home self-testing. Early detection can have a profound impact on treatment outcomes and mitigation of damage for a number of illnesses. Points of care systems are viewed as integrated systems that can make state-of-the-art technology platforms accessible to a large population pool [2]. However,

the vast majority of medical diagnostics is still conducted in clinical laboratories and with the use of large equipment. Many hurdles need to be overcome before new analytical tools can be widely accepted in medical practice [3]. Microfluidics provides the ability to analyze small volumes of sample and minimize costly reagent consumption, automate sample preparation, and reduce processing time, but it is still fraught with challenges. These challenges include developing low-cost fluidic chip manufacturing methods, providing good interfaces to the macro-world, minimizing non-specific analyte/wall interactions (due to the high surface-to-volume ratio associated with microfluidics), developing materials that accommodate the optical readout phases of the assay, and complete integration of peripheral components to produce autonomous systems appropriate for point-of-care testing [4].

* Corresponding author.

E-mail address: tony.garcia@asu.edu (A.A. García).

Since microfluidics holds promise as a key component in the next generation of point of care diagnostic devices, it is useful to review the major formats being developed. Two basic paradigms in microfluidics are continuous flow [5] and digital microfluidics [6] where fluid is handled in unit-sized packets. Most digital microfluidics systems place drops in an immiscible liquid environment. Actuation mechanisms include electro-wetting [7,8] and magnetic manipulation of aqueous droplets suspended in silicone oil filled microchannels driven by magnetic microparticles [9]. Rectified motion of drops in air (on gradient sources induced by vibration) has also been investigated [10]. There is no doubt that this area of research is still expanding with an eye towards simplicity, versatility, and integration with the latest sensing and detection technology. With these ideas in mind, our research group has also been developing a new method to manipulate discrete drops of aqueous and biological fluids.

We recently reported a novel method to displace, coalesce, split, and analyze paramagnetic particle-containing aqueous drops in air using flat, non-patterned silicon nanowire superhydrophobic surfaces with the only driving force being magnetic fields [11]. Discrete magnetic microfluidics, or digital magnetofluidics, is a technique in which aqueous and biological fluids drops can be moved in air over a superhydrophobic surface by magnetic force. Briefly, aqueous and biological fluid drops with iron microparticle concentrations of approximately 5% can be moved on a silicon nanowire (Si NW) superhydrophobic surface via magnetic forces (Fig. 1). Iron microparticles were coated with polyxiloxane in order to prevent oxidation in aqueous environments as described in Ref. [12], and then added to the drops. Si NW superhydrophobic surfaces were created by a CVD process [13–15], followed by chemical coating with a fluorinated hydrocarbon. Basic drop handling operations through digital magnetofluidics with biological fluids drops, such as bovine serum albumin solutions, plasma, and serum have also been demonstrated [16]. This technique has been successfully coupled to electrochemical detection methods for quantitative dopamine and glucose analyses [17]. The digital magnetofluidic format has a number of advantages since sample droplets can be simply handled individually in air while maintaining minimal contact with the surface (Fig. 2a) thus drastically reducing wall interactions.

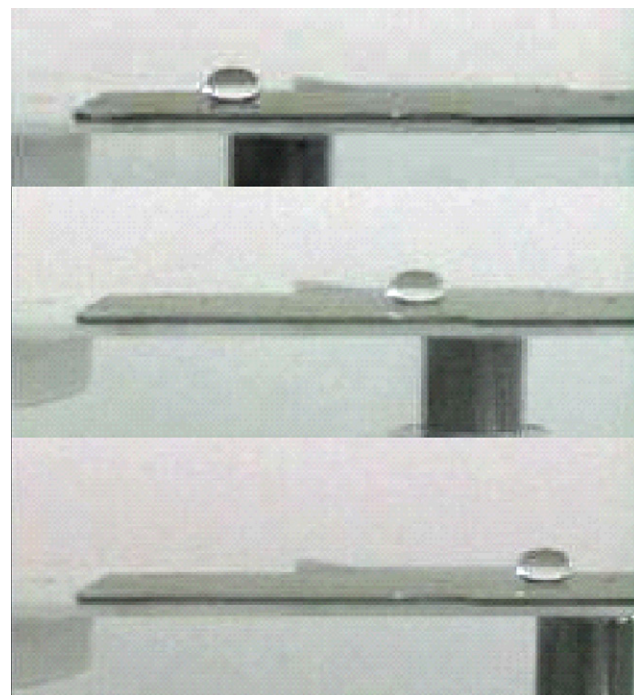


Fig. 1. Sequence of frames from a video of a 30 μL water drop moving from left to right on a silicon nanowire superhydrophobic surface with an iron particle concentration of 5% by the action of a permanent magnet below the surface.

In this study, we report observations of digital magnetofluidics on another superhydrophobic surface based on crystallization of low-density polyethylene (LDPE). Since LDPE and Si NW surfaces have very different morphologies and chemistries, it is important to compare and contrast how drops can be moved on these surfaces through the action of digital magnetofluidics.

2. Experimental

2.1. Si nanowire superhydrophobic surfaces

Si(100) n-type wafers used for silicon nanowire growth were degreased by rinsing in acetone for 10 min followed by a methanol rinse for another 10 min. They were then etched with a 10:1 buffered 48% HF solution for 10 min to remove the oxide

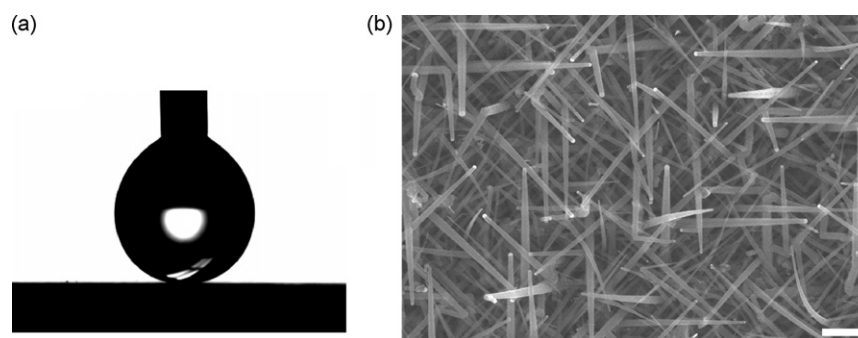


Fig. 2. Silicon nanowire superhydrophobic surface. (a) Water drop showing a static contact angle higher than 170° . The drop is held by the pipette tip to prevent it from rolling off the surface. (b) Top view SEM of the nanowire surface. On the SEM image it is possible to distinguish the gold-capped nanowires with different directions covering the surface. The nanowire grow conditions were 460°C , 1 Torr, 18 min, and the nanowire average length was $2.5\ \mu\text{m}$.

layer and dried under flowing nitrogen. A 2 nm gold film was thermally evaporated onto hydrogen terminated Si(1 0 0) substrates in a vacuum of 10^{-7} Torr at room temperature to create gold nanodots. Silicon nanowires were grown on the gold nanodots via catalytic vapor–liquid–solid (VLS) growth in a quartz lamp heated, low-pressure chemical vapor deposition (LPCVD) system. The wafer was supported by a SiC-coated graphite susceptor. The wafer was annealed first in hydrogen (3000 SCCM) at the growth temperature for 30 min, followed by outgassing, and at 570 °C for 5 min to promote the formation of Au–Si eutectic droplets. A hydrogen atmosphere with 5% SiH₄ was introduced at a flow rate of 400 SCCM. Nanowires were grown under 2.5 W RF plasma conditions at a temperature and pressure of 460 °C and 1.0 Torr for 20 min. A Hitachi-S-4700-II field emission scanning electron microscope was used to obtain high-resolution images from which length and thickness of the nanowires were determined. A 10 keV electron beam and 6 mm working distance were used to obtain images in low energy secondary electron imaging mode.

Fig. 2b shows a top view SEM image of the Si NW surface grown under plasma conditions at 460 °C. Silicon nanowires predominantly grow in $\langle 1\ 1\ 0 \rangle$ and $\langle 1\ 1\ 1 \rangle$ orientations. When viewed from above, the $\langle 1\ 1\ 0 \rangle$ oriented nanowires are at a 45° angle with respect to both the horizontal and vertical axes, while the $\langle 1\ 1\ 1 \rangle$ oriented nanowires are parallel to the horizontal and vertical axes. The average length of the nanowires is 2.5 μm.

The Si NW surface was cleaned in a UV ozone cleaner for 30 min. The sample was immediately rinsed with DI water and heated at 140 °C for 10–15 min to dry the surface. Cleaned Si NW surfaces were incubated in a 0.1% aliquot of 1H, 1H, 2H, 2H-perfluorooctyltrichlorosilane (PFOS) solution in double-distilled toluene for 30 min, then twice-rinsed with toluene. Then, the sample was dried at 140 °C for 15 min and stored in a Petri dish at room temperature.

2.2. Low-density polyethylene superhydrophobic surfaces

Superhydrophobic LDPE surfaces were prepared by adapting the method of Lu et al. [18]. LDPE was chosen as the substrate for its inherent hydrophobicity, low cost, and flexibility. A 1.59 mm thick commercial-grade LDPE sheet was purchased from McMaster-Carr (Los Angeles, CA). LDPE crystals were grown from LDPE pellets (Sigma–Aldrich, St. Louis, MO) with a melt index of 2.50 g/min at 190 °C. The pellets were dissolved in xylene (isomers plus ethylbenzene, reagent grade, Sigma–Aldrich) and methyl ethyl ketone (MEK) (reagent grade, J. T. Baker, Phillipsburg, NJ). The LDPE sheet was cut into 61 mm × 99 mm rectangles to fit into an aluminum solvent-casting fixture. The rectangular samples were lightly abraded and cleaned with acetone before being clamped on the fixture. The LDPE pellets, xylene, and MEK were used without additional preparation. Xylene solvent and LDPE pellets (at a concentration of 30 mg/mL) were placed in a flask and immersed in a water bath at 92 °C. After the LDPE had fully dissolved (approximately 35 min), MEK (a non-solvent for LDPE) was added to the flask at a ratio of 55:45

xylene:MEK. The addition of a non-solvent to the solvent-plastic solution was shown by Erbil et al. [19] to increase surface roughness and aqueous drop contact angle for solvent-cast polypropylene. Our research has shown that a similar result is achieved for solvent-cast LDPE using MEK as the non-solvent. The addition of the MEK caused the solution to immediately turn cloudy due to crystallization, but after several minutes of gentle swirling the solution cleared. At this point the water bath temperature was decreased to 80 °C and the solution was held at that temperature for an additional 90 min to promote controlled crystallization. Next, 5 mL of solution was carefully withdrawn and pipetted into the fixture (resulting in a surface concentration on the LDPE sheet of 0.090 mL of solution/cm², or 2.7 mg of crystals/cm²). The fixture was gently rocked to level the solution, and then placed in an enclosed box and kept in a fume hood to dry overnight.

2.3. Magnetic movement

Aqueous drops containing paramagnetic iron particles (6–9 μm, Fluka) were pipetted onto the Si NW and LDPE superhydrophobic surfaces. The iron particles were coated with polysiloxane to prevent oxidation as described in Ref. [12]. Drop movement was accomplished by displacing a cylindrical NdFeB bar magnet, which the drop being positioned directly below the superhydrophobic surface (for horizontal movement) (Fig. 4a) or on the opposite face of the surface (for vertical and upside-down movement) (Fig. 4b–c).

2.4. Static contact angle measurements

Contact angle measurements of water drops on both silicon nanowire and low-density polyethylene super hydrophobic surfaces were made by the sessile drop method, adjusting the drop volume from the top of the drop, with a Ramé–Hart (Mountain Lakes, NJ) NRL Contact Angle Goniometer, model 100-00.

3. Results and discussion

One major goal of our research is to find ways to manipulate biological fluids without the use of a container or channels. Our early studies were designed specifically with the intent of carefully controlling surface properties in order to generate droplet movement. With that goal in mind, Silicon nanowire (Si NW) superhydrophobic surfaces were prepared using vapor–liquid–solid (VLS) growth systems to create high aspect ratio nanowires of various diameters, spacing, and lengths. The nanowire substrates were rendered hydrophobic by covalently applying a perfluorinated hydrocarbon coating to the entire surface. This combination of topography and hydrophobic coating resulted in surfaces where drop contact angles measurements gave advancing contact angles close to 180° (Fig. 2a), with no detectable difference between advancing and receding contact angles. The Si NW superhydrophobic surfaces are macroscopically smooth, however, they exhibit multi-dimensional, random roughness at a small scale (Fig. 2b). The

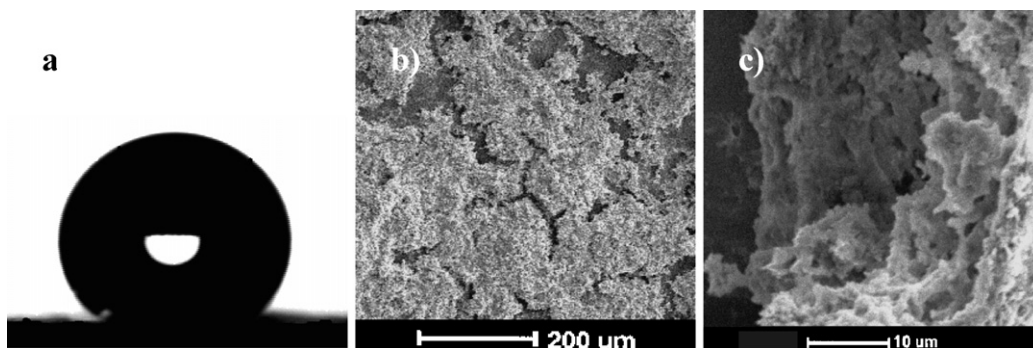


Fig. 3. Low-density polyethylene surfaces (LDPE). (a) Water drop on LDPE superhydrophobic surface, showing a static contact angle of approximately 150° . (b) Top view SEM of $50\times$ magnified image shows that the polyethylene crystals do not cover the surface homogeneously, however, the sample is still superhydrophobic. (c) Top view SEM of $1500\times$ magnified image shows the floral-like low-density polyethylene structures that cover the polyethylene slab, making the surface superhydrophobic by a combination of multidimensional surface roughness and the intrinsic hydrophobicity of polyethylene.

smallest feature length scale is about 20 nm which corresponds to the nanowire diameters. The next largest length scale is the separation distance between nanowires, which ranged from 60 to 100 nm. The largest roughness length scale is represented by the nanowire height, of approximately $2\ \mu\text{m}$. These different feature/roughness length scales give rise to the mechanism for water repellency in Lotus leaf-like structures which is the presence of air pockets underneath the liquid [20,21].

Si NW superhydrophobic surfaces have shown to be excellent substrates for movement of drops even for solutions with protein concentrations similar to those found in blood. We have also observed that drops of whole blood, serum, plasma, urine, and saliva are repelled by Si NW superhydrophobic surfaces. While this surface shows excellent promise as a platform for biological fluid microfluidics, we are interested in broadening the types of materials that could support digital magnetofluidics. For this reason, most recently, we have shifted our attention to the use of low-density polyethylene (LDPE) superhydrophobic surfaces. LDPE is intrinsically hydrophobic, and a more commercially relevant material. Polymer surfaces are in general attractive because of their flexibility and the ease in which complex structures can be formed. Through solvent crystallization, LDPE superhydrophobic surfaces can be made very quickly and inexpensively in large slabs.

Contact angles on LDPE superhydrophobic surfaces are approximately 148° when measured on a static drop, 152° for

an advancing drop and 138° for a receding drop. LDPE solvent crystallization produces floral-like structures with multidimensional roughness. Macroscopically, LDPE superhydrophobic surfaces appear very rough. The largest feature length scale (approximately $100\ \mu\text{m}$) is due to cracks that appear between the crystallized areas (Fig. 3b). At the complex floral structure level, features of 1 and $10\ \mu\text{m}$ are also found, and significant roughness at the nanoscale-level should also be present.

The mechanism for water repellency of superhydrophobic surfaces is given by Wenzel's law [22], $\cos \Theta^* = r \cos \Theta$; where Θ^* is the resulting contact angle for a surface with a given roughness parameter r , and the contact angle Θ is the value measured for a smooth surface. The value of r is the ratio of the real surface area divided by the projected flat surface area [20]. From values of water on pristine low-density polyethylene films of 93° [23] and an estimated Wenzel contact angle of 147° , r can be estimated as approximately 16 for the LDPE surfaces.

Drops of sizes up to $4\ \mu\text{l}$, with iron-microparticle concentration of 5% can be moved through digital microfluidics in three-dimensions (Fig. 4). Up to now, digital microfluidics systems have been confined to motion in a 2-D channel or a 2-D surface. Yet, 3-D movement is important because more compact devices can be fabricated and more sophisticated subsystems for detection and processing would be possible. Three-dimensional motion may also allow for more flexibility

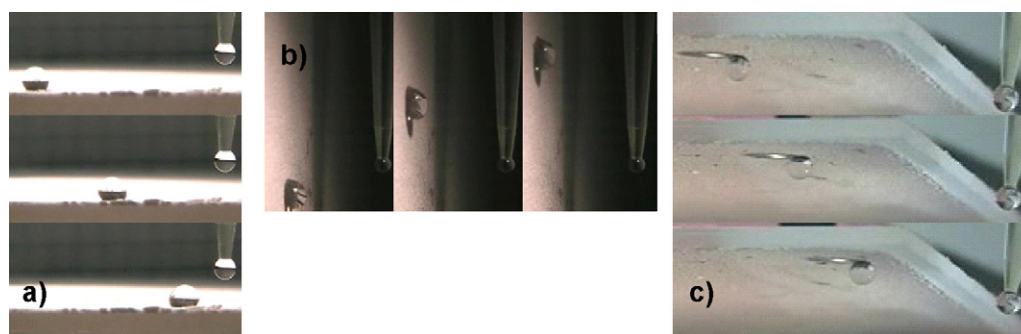


Fig. 4. Sequence of frames from a video showing movement of water drops in three-dimensions, on a low-density polyethylene surface. (a) Drop moving from right to left on a horizontal surface. (b) Drop moving upwards along a vertical surface. (c) Drop moving from left to right on an upside-down surface. All drops contain 5 wt.% siloxane-coated, iron microparticles. On the right of all frames a pendant drop from a pipette tip is shown as a gravity reference.

when employing multiple sensor elements since they do not have to be integrated with the substrate as would be the case for a planar configuration. We are currently involved in studies to thoroughly investigate the movement of drops on each type of surface. At this point, several qualitative observations can be made. First, Si NW superhydrophobic surfaces provide very little resistance to movement; and thus drops can be moved on these surfaces at the speeds of up to 7 cm/s [11]. Secondly, LDPE surfaces provide higher resistance to movement and drops can be moved only when higher concentrations of magnetic particles are added (5–10%) or smaller drops are used. Thirdly, LDPE superhydrophobic surfaces are more robust than Si NW surfaces and continue to give consistent performance over repetitive drop movement cycles. Finally, superparamagnetic particles do not seem to get caught in the LDPE surface features, whereas there is visual and contact angle evidence indicating that they become embedded in Si NW surfaces.

At this point, we also believe that the LDPE surfaces can be better designed to reach the same performance characteristics seen in the Si NW surfaces. Erbil et al. [19] note that polypropylene superhydrophobic surfaces can yield higher contact angles. Also, better control of LDPE crystal growth [18] should also increase contact angles. It is hypothesized that a higher contact angle will result in easier drop movement with plastic surfaces requiring lower concentrations of magnetic particles.

4. Conclusions

Superhydrophobic surfaces created by LDPE crystallization can be used in digital magnetofluidics. While their performance does not quite match Si NW surfaces, improvements in crystal structure or a switch to polypropylene could lead to plastic superhydrophobic surfaces that rival silicon nanowire performance. The strength of Si NW surfaces in this application is due to dense, high aspect ratio structures which yield very high contact angles and avoid receding angle pinning spots. Overall, Si NW surfaces provide a lower resistance to drop movement using magnetic particles, and larger drops or lower concentrations of paramagnetic particles are sufficient for these surfaces. Interestingly, capillary forces in digital magnetofluidics are strong enough to allow drop movement vertically and upside-down on superhydrophobic surfaces for drops volumes up to 4 μl on low-density polyethylene surfaces. This demonstration of 3-D microfluidic movement opens the door for more compact devices and an expanded array of sensing elements.

Acknowledgements

We want to thank Dr. N. Newman and H. Liu (School Of Materials, ASU) for their collaboration with magnetic measurements. This work was supported in part by the

Interdisciplinary Network of Emerging Science and Technologies (INEST) and More Graduate Education at Mountain States Alliance (MGE@MSA). In addition, financial support (for D.Y., P.A. and S.T.P.) by the National Science Foundation (DMR-0413523), and for M.A.R. and P.D.G. by M.E.C. (FIS2005-0134) and by C.A.M (S-0505/MAT/0227) is gratefully acknowledged.

References

- [1] S. Daunert, Analytical and bioanalytical chemistry in white waters: 2006 and beyond, *Anal. Bioanal. Chem.* 384 (1) (2006) 1618–2642.
- [2] J. Wang, Electrochemical biosensors: towards point-of-care cancer diagnostics, *Biosens. Bioelectron.* 21 (10) (2006) 1887–1892.
- [3] E.P. Kartalov, Multiplexed microfluidic immunoassays for point-of-care in vitro diagnostics, *IVDT* (2006) 55.
- [4] C. Situma, M. Hashimoto, S.A. Soper, Merging microfluidics with microarray-based bioassays, *Biomol. Eng.* 23 (5) (2006) 213–231.
- [5] A. Manz, N. Graber, H.M. Widmer, Miniaturized total chemical analysis systems: a novel concept for chemical sensing, *Sens. Actuat. B: Chem.* 1 (1–6) (1990) 244–248.
- [6] M.G. Pollack, R.B. Fair, A.D. Shenderov, Electrowetting-based actuation of liquid droplets for microfluidic applications, *Appl. Phys. Lett.* 77 (11) (2000) 1725–1726.
- [7] S.Y. Chou, C. Keimel, J. Gu, Ultrafast and direct imprint of nanostructures in silicon, *Nature* 417 (6891) (2002) 835–837.
- [8] P. Paik, V.K. Pamula, R.B. Fair, Rapid droplet mixers for digital microfluidic systems, *Lab Chip* 3 (2003) 253–259.
- [9] U. Lehmann, et al., Two-dimensional magnetic manipulation of microdroplets on a chip as a platform for bioanalytical applications, *Sens. Actuat. B: Chem.* 117 (2) (2006) 457–463.
- [10] S. Daniel, M.K. Chaudhury, Rectified motion of liquid drops on gradient surfaces induced by vibration, *Langmuir* 18 (2002) 3404–3407.
- [11] A. Egatz-Gomez, et al., Discrete magnetic microfluidics, *Appl. Phys. Lett.* 89 (3) (2006) 034106.
- [12] H. Pu, F. Jiang, Z. Yang, Studies on preparation and chemical stability of reduced iron particles encapsulated with polysiloxane nano-films, *Mater. Lett.* 60 (1) (2006) 94–97.
- [13] J.W. Dailey, et al., Vapor-liquid-solid growth of germanium nanostructures on silicon, *J. Appl. Phys.* 96 (12) (2004) 7556–7567.
- [14] T. Clement, et al., In situ studies of semiconductor nanowire growth using optical reflectometry, *Appl. Phys. Lett.* 89 (16) (2006) 163125.
- [15] P. Aella, S. Ingole, W.T. Petuskey, S.T. Picraux, Influence of Plasma Stimulation on Si Nanowire Nucleation and Orientation Dependence, *Advanced Materials* 19 (2007) 2603–2607.
- [16] A.A. García, et al., Magnetic movement of biological fluid droplets, *J. Magn. Magn. Mater.* 311 (2007) 238–243.
- [17] S. Lindsay, et al., Magnetic digital microfluidics with electrochemical detection, *Analyst* 132 (2007) 412–416.
- [18] X. Lu, C. Zhang, Y. Han, Low-density polyethylene superhydrophobic surface by control of its crystallization behavior, *Macromol. Rapid Commun.* 25 (18) (2004) 1606–1610.
- [19] H.Y. Erbil, et al., Transformation of a simple plastic into a superhydrophobic surface, *Science* (2003) 1377–1380.
- [20] A. Otten, S. Herminghaus, How plants keep dry: a physicist's point of view, *Langmuir* 20 (6) (2004) 2405–2408.
- [21] D. Quere, Fakir droplets, *Nat. Mater.* 1 (1) (2002) 14–15.
- [22] R.N. Wenzel, Surface roughness and contact angle (letter)[J], *J. Phys. Colloid. Chem.* 53 (1) (1949) 466–471.
- [23] V. Svorcik, et al., Modification of surface properties of high and low-density polyethylene by Ar plasma discharge, *Polym. Deg. Stab.* 91 (6) (2006) 1219–1225.